

Enhancing Light Emission of ZnO-Nanofilm/Si-Micropillar Heterostructure Arrays by Piezo-Phototronic Effect

Xiaoyi Li, Mengxiao Chen, Ruomeng Yu, Taiping Zhang, Dongsheng Song, Renrong Liang, Qinglin Zhang, Shaobo Cheng, Lin Dong, Anlian Pan, Zhong Lin Wang,* Jing Zhu,* and Caofeng Pan*

Silicon-based light-emitting diode (LED) arrays as strain sensors to present force/pressure distributions through the light emission intensities could revolutionize the current technologies for the e-skin of the robotics and the human-machine interfaces. In this work, n-ZnO nanofilm/p-Si micropillar heterostructure (ZSH) LEDs array are designed to achieve white light emissions at room temperature, featuring with emission peaks in both visible and near-infrared regions. By applying a strain onto the top of the ZSH LEDs, the light emission intensity of ZSH LEDs array was enhanced by 120% under -0.05% compressive strains. The reason is that the strain-induced piezoelectric polarization charges at the interface between Si and ZnO can be utilized to modify the energy band structure of ZnO and thus tune/control the transport, separation, and/or recombination processes of photo-generated carriers. It is called piezo-phototronic effect. A pressure map can be created by reading out in parallel the change of the electroluminescent intensities from all the pixels in the near future. This research not only introduces a novel approach to fabricate Si-based light-emitting components with high performances but also may be a great step toward digital imaging of mechanical signals using optical means, having potential applications in artificial skin, touch pad technology, personalized signatures, bioimaging and optical Microelectromechanical Systems (MEMS), and even smart skin. Moreover, these technologies are totally compatible with the dominate silicon microelectronic industry, which means large-scale integrated device could be easily achieved for future assembling in silicon-based photonic integrated circuits (PIC) and optical communication systems.

PIC have been investigated for decades to process information imposed on optical signals as an essential component for fiber-optic communications,^[1] biomedical technology,^[2] photonic computing,^[3] and many more applications.^[4] Apart from indium phosphide (InP), which is the most commercialized material platform for PIC,^[5] Si has been extensively developed as an alternative due to its conceivable prospect to be integrated with the existing well-developed Si technologies in various fields.^[1] However, it has been challenging to build a high-efficiency light-emitting component with Si, since the indirect band gap and low carrier mobility of silicon lead to low light-emitting efficiency and poor optoelectronic performances.^[6] Tremendous efforts have been devoted to improving the electroluminescence (EL) properties of silicon through structure modifications (porous silicon, etc.),^[7] doping with special elements (e.g., Er)^[8] and energy band engineering.^[9] Particularly, it has been reported that forming heterostructures between Si and semiconducting materials, such as GaN and ZnO,^[10] is one of the most promising solution to fabricate high-efficient light-emitting component based on silicon.

In this work, we designed and fabricated ordered LED array through inductive coupled plasma (ICP) etching of Si wafer and ZnO thin film to produce ZSH for light emissions at room temperature. White light LEDs array are achieved and characterized by EL spectrum with peaks in both visible and near-infrared regions. As one of the wurtzite family materials with noncentral symmetric crystal structure, ZnO possesses piezoelectric property with *c*-axis polarization under strain. By pressing the ZSH LEDs array, strain-induced piezoelectric

X. Li, D. Song, S. Cheng, Prof. J. Zhu
National Center for Electron Microscopy in Beijing
School of Materials Science and Engineering
The State Key Laboratory of New Ceramics
and Fine Processing
Key Laboratory of Advanced Materials (MOE)
Tsinghua University
Beijing 100084, P. R. China
E-mail: jzhu@mail.tsinghua.edu.cn
X. Li, M. Chen, Dr. T. Zhang, Prof. L. Dong,
Prof. Z. L. Wang, Prof. C. Pan
Beijing Institute of Nanoenergy and Nanosystems
Chinese Academy of Sciences
Beijing, China
E-mail: zlwang@gatech.edu; cfpan@binn.cas.cn

X. Li, S. Cheng, Prof. J. Zhu
Center for Nano and Micro Mechanics
Tsinghua University
Beijing 100084, China
R. Yu, Prof. Z. L. Wang
School of Materials Science and Engineering
Georgia Institute of Technology
Atlanta, GA 30332-0245, USA
Prof. R. Liang
Institute of Microelectronics
Tsinghua University
Beijing 100084, China
Prof. Q. Zhang, Prof. A. Pan
Key Laboratory for Micro-Nano Physics
and Technology of Hunan Province
Hunan University
Changsha, Hunan 410082, China



DOI: 10.1002/adma.201501121

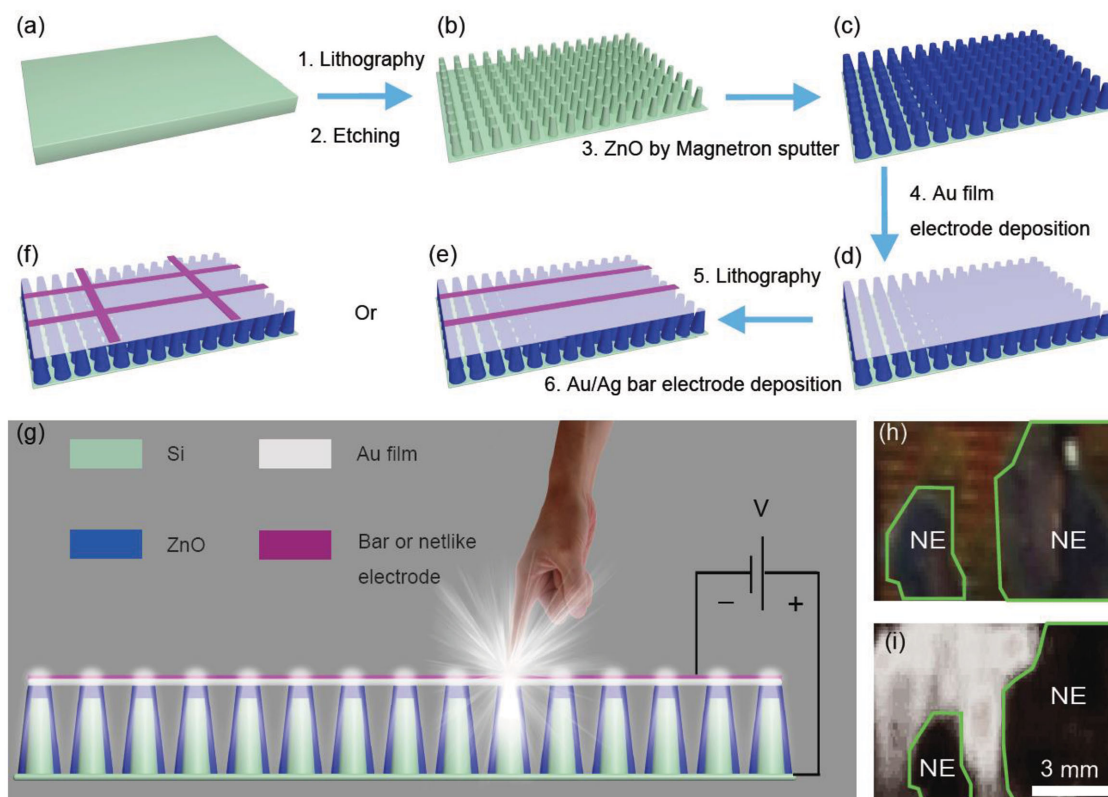


Figure 1. Fabrication processes of ZSH LEDs array. a–f) Schematic illustration of the fabrication process of ZnO-nanofilm/Si-micropillar LED array. g) Schematic demonstration of piezo-phototronic effect enhanced light emissions of ZSH LEDs array under strain. h) An optical image of the as-fabricated device. i) An optical image of the device operating at a biased voltage of 10 V. The negative electrode (NE) is marked with a green polygon in (h) and (i).

polarization charges presented at the vicinity of local hetero-junction have been utilized to modify the energy band structure of ZnO and thus tune/control the transport, separation, and recombination processes of photo-generated carriers. This is the piezo-phototronic effect.^[11] The light emission intensity of ZSH LEDs array was enhanced by 120% under -0.05% compressive strains. A pressure map can be created in the foreseeable future by reading out in parallel the change of the electroluminescent intensities from all the pixels. This research not only introduces a novel approach to fabricate Si-based light-emitting components with high performances but also may be a great step toward digital imaging of mechanical signals using optical means, having potential applications in artificial skin, touch pad technology, personalized signatures, bioimaging and optical MEMS, and even smart skin. Moreover, these technologies are totally compatible with the dominate silicon micro-electronic industry, which means large-scale integrated device could be easily achieved for future assembling in silicon-based PIC becomes feasible for potential applications.

The fabrication process of ZSH LEDs array is schematically illustrated in **Figure 1**. Cleaned p-type Si wafers ($\rho \approx 0.01 \Omega \text{ cm}$) were immersed into hydrofluoric acid (1%) for 2 min before spin coated by patterned photoresist through photolithography. Different from the method of chemical etching,^[12] ICP etching was then introduced to produce micropillar structures (Figure 1b), followed by magnetron sputtering of n-type ZnO nanofilm

(Figure 1c) and Ag/Au thin film electrodes (Figure 1d). Finally, the bar electrodes (Figure 1e) or network electrodes (Figure 1f) were fabricated on top of the whole device. Detailed fabrication process can be found in the Experimental Section. Upon straining, the touched part of ZSH LEDs array will emit brighter than others as schematically shown in Figure 1g, which can be used as a strain/pressure mapping system with high resolution in the future. The optical image of a typical device is presented in Figure 1h, together with another image showing the device operating under a biased voltage of 10 V (Figure 1i).

ZnO/Si micropillar heterostructures are carefully characterized by electron microscopy as shown in **Figure 2**. Top and tilted view scanning electron microscopy (SEM) images of Si micropillars are shown in Figure 2a, indicating the height of 5 μm , the bottom diameter of 4.1 μm , and the top diameter of 1.7 μm for Si micropillar structures. A layer of ZnO nanofilm is uniformly deposited to completely cover the Si micropillars as shown in Figure 2b. High-magnification SEM images of ZnO nanofilm, presented in Figure S2 (Supporting Information), demonstrate that the ZnO nanofilm consists of many crystals. Two different types of top electrodes, bar electrodes, and network electrodes are demonstrated by SEM images presented in Figure 2c,d, respectively. The Si–SiO₂–ZnO interface is characterized by high-resolution transmission electron microscopy (TEM) image as shown in Figure 2e, from which a thin layer of amorphous SiO₂ is observed with thickness of 3 nm. The

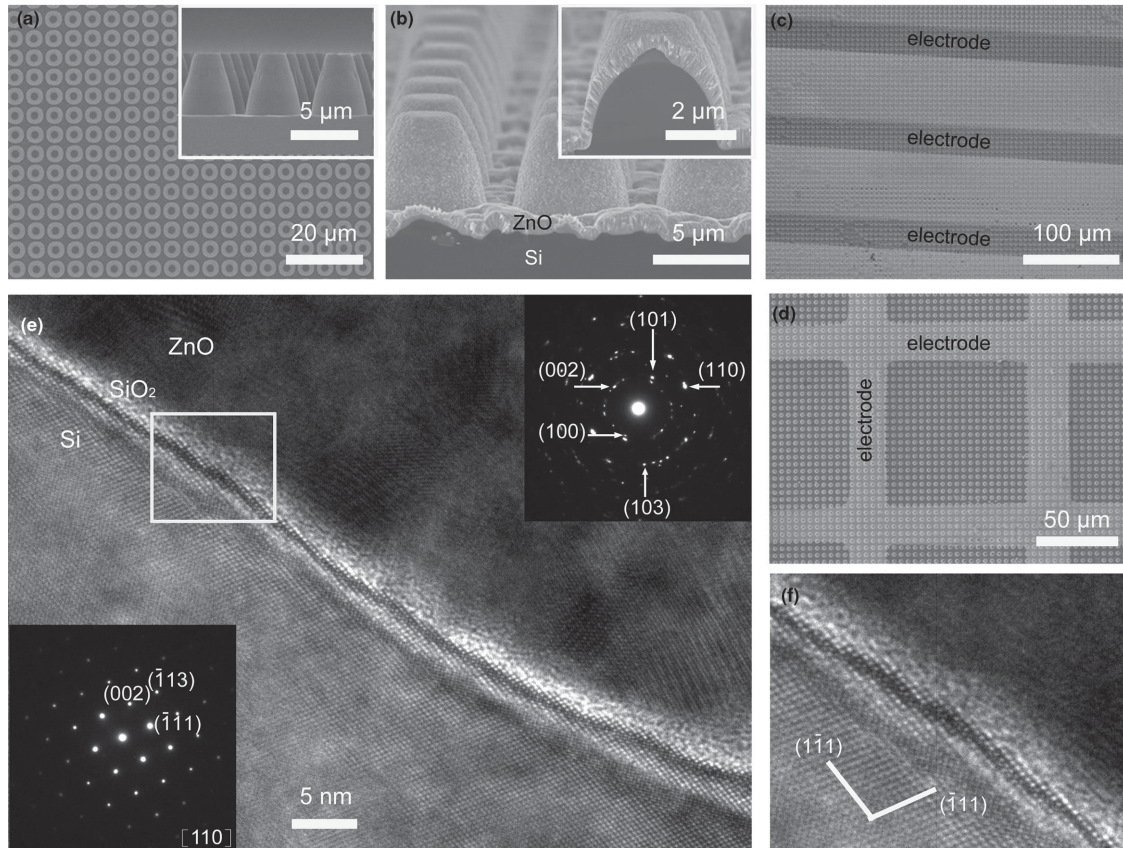


Figure 2. Structure characterizations of ZSH LEDs array. a) Top view and side view (inset) SEM images of Si micropillars. b) Cross-sectional SEM images of ZnO covered Si micropillars. c, d) SEM images of the as-fabricated device with c) bar electrodes and d) network electrodes. e) HRTEM image of Si-SiO₂-ZnO interface. The insets are SAED patterns of Si (left bottom corner) and ZnO (right top corner). f) HRTEM image derived from the selected area marked in (e).

selected-area electron diffraction (SAED) pattern of Si (inset of Figure 2e, left) confirms its single crystalline, while the SAED pattern of ZnO nanofilm (inset of Figure 2e, right) indicates the presence of different crystallographic directions. Figure 2f is the HRTEM image derived from the selected area marked in Figure 2e, revealing the existence of high index atomic steps at the interface, which leads to an increase in band gap energy at the edge.^[13]

Light emissions of ZSH LEDs array device at a biased voltage of 10 V are recorded and presented in Figure 3a,b, corresponding to the device fabricated with network electrodes and bar electrodes, respectively. Insets of Figure 3a,b are the corresponding optical images under ambient illumination. By looking at a high-magnification light-emitting image of the device with bar-electrodes as shown in Figure 3c, emission intensity difference among individual micropillar LEDs is observed as a result of various defects concentration on the surface of Si micropillars and nonuniform serial contact resistances distributions of top electrode.^[14] Therefore, light emissions with stronger intensity are observed from micropillar LEDs locating closer to the electrodes due to less contact resistance. Better performances and more uniform as the bar electrodes with network electrodes, since the current crowding effect and serial contact resistances issue are effectively resolved with more advanced structure designs. The line

profile of emission intensity derived from eight typical ZSH LEDs (marked in Figure 3c) is investigated and summarized in Figure 3d. The center-to-center distance between two adjacent LEDs is obtained as 5.2 μm , corresponding to a pixel resolution of 4885 dpi. If the ZSH LEDs array could be used as a strain/pressure mapping system, the actual resolution would be 2.6 μm , as defined by the full-width at half-maximum of the emission pixels. No crosstalk is observed from neighboring pixels, indicating a reliable resolution of LED arrays.

The EL emission spectra of a typical device is obtained under different injection currents (0.2, 0.4, 0.6, 0.8, 1.0, 1.1, 1.2, and 1.3 A) at room temperature, as shown in Figure 3e. It is obvious that the EL intensity increases with the injection current, as expected from the band-bending model of a p-n junction.^[15] Besides, the peak positions in spectra derived under injection current from 0.2 to 1 A are similar to one another, while under injection current larger than 1 A, the peak near 820 nm starts to appear and increase significantly as increasing the injection current. To better understand the physical process of light emissions, peak deconvolution with Gaussian functions is conducted to the broad spectrum at the injection current of 1.3 A as shown in Figure 3f. Five distinct bands are derived from the deconvolution and each emission band corresponds to a particular recombination process as elaborated in the following. Since the thickness of SiO₂ layer is ≈ 3 nm (Figure 2e), carriers can

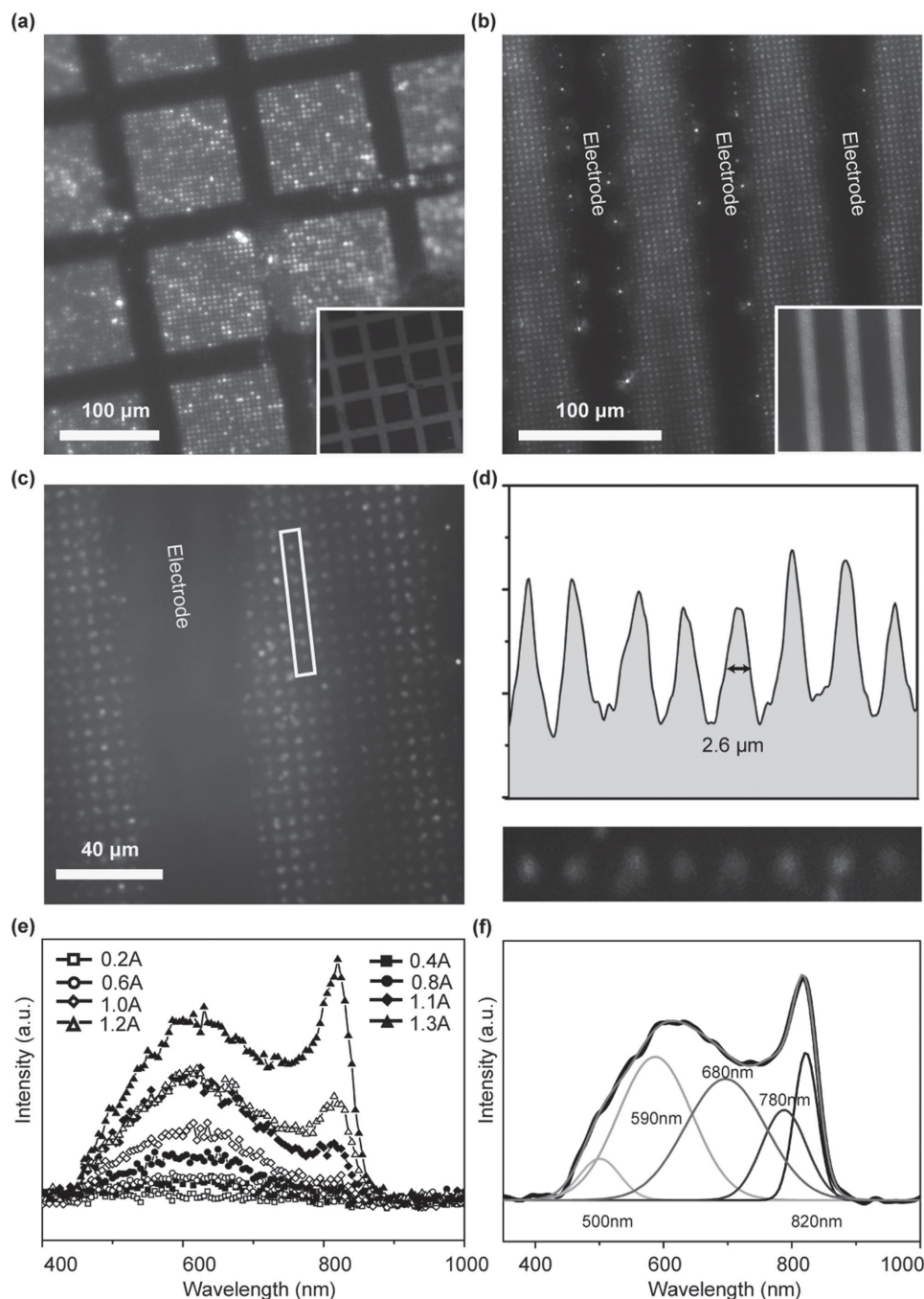


Figure 3. Light-emitting performances of the device. a,b) Optical images of the as-fabricated device with a) network electrodes and b) bar electrodes operating under 10 V biased voltage. c) High-magnification optical image of the device with bar electrodes operating under 10 V biased voltage. d) Line profile of the emissions intensity derived from eight typical LEDs marked with a white rectangle in (c). e) EL spectra of the as-fabricated device operating under different injection currents at room temperature. f) Peak deconvolution of the broad spectrum with Gaussian functions at the injection current of 1.3 A.

tunnel through the barrier and the electrons from ZnO recombine with the holes from Si.^[7] The peak (≈ 500 nm) and the peak (≈ 590 nm) in Figure 3f are therefore associated with the defects emissions in ZnO nanofilm.^[7,10,16] Due to the presence of high index atomic steps at the edge of Si micropillar (Figure 2f) and nanostructures at the heterojunction interface (Figure S1a,b, Supporting Information), the energy band gap of Si near the

ZnO/Si pn junction is larger than that of bulk Si,^[13] which is related to the peak of 680 nm.^[9,17] The near-infrared emission centered at around 780 nm comes from the Si microstructure such as the micropillar arrays and nanopits on the micropillar surface (Figure S1c,d, Supporting Information).^[17,18] Within the Si-SiO₂ interface layer, there are a large number of interface traps and defect levels from the broken bonds and impurities

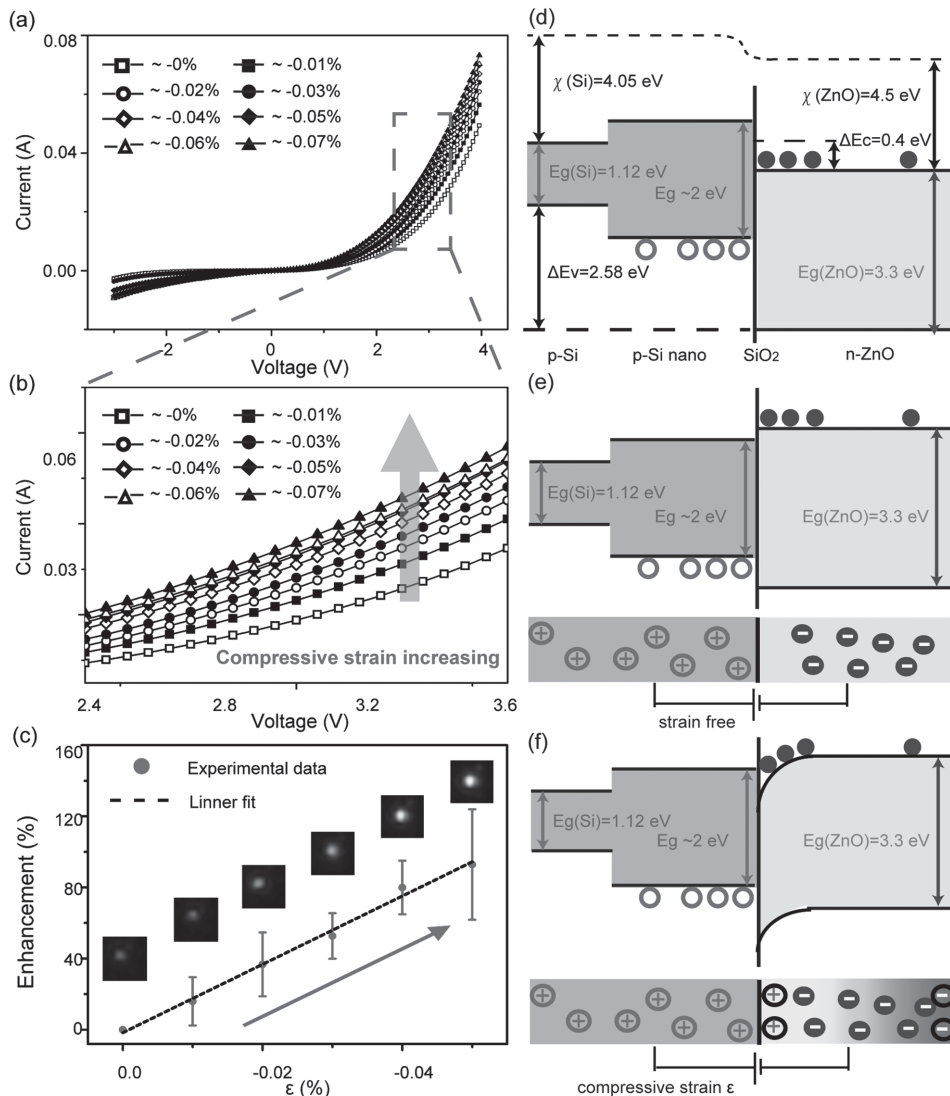


Figure 4. Piezo-phototronic effect enhancements and working mechanism. a, b) *I*-*V* characteristics of the device operating under various applied strains. c) Enhancement factor *E* versus strains ϵ , together with the corresponding images of light emissions. d, e, f) Energy band diagrams of ZSH LEDs array under (d) no strains nor bias voltage; e) no strain and a bias voltage; and f) compressive strains and a bias voltage.

of Si crystals. The orange line peaked near 820 nm is attributed to the radiative recombination of carriers at the interface between Si and SiO₂.^[19] As a comparison, EL spectra of devices fabricated without Si micropillars were also measured and presented in Figure S3a (Supporting Information), the obvious differences in spectra are attributed to field enhancement effect of silicon micro- and nanostructures.^[6]

The dependence of *I*-*V* characteristics on the externally applied strains is presented in Figure 4a, b to indicate the light-emission enhancements of piezo-phototronic effect on ZSH LEDs array.^[20] The corresponding experimental setups are presented in Figure S4 (Supporting Information). It is clear to conclude that, at the same biased voltage, the current increases obviously with the externally applied compressive strains, indicating the control of piezo-phototronic effect over the light emissions of ZnO/Si LED. A better understanding of the enhanced performances by piezo-phototronic effect is

derived by defining the enhancement factor of LED intensity *E* as $E = (I_\epsilon - I_0)/I_0$, as shown in Figure 4c. It is obvious that the enhancement factor *E* is approximately linearly dependent on the external strains, with the maximum value of 120% at a compressive strain of -0.05%.^[21] Therefore, piezo-phototronic effect successfully improved the efficiency of Si-based light-emitting components significantly to overcome the indirect band structure and low carrier mobility of silicon.

The physical mechanism of piezo-phototronic effect enhancements is carefully illustrated by utilizing schematic band diagrams of ZnO-Si heterostructure as shown in Figure 4d-f. Upon compressively straining, the relative displacement of centers of cations and anions occurs within ZnO due to its noncentral symmetry.^[22] The textured ZnO nanofilm is +*c*-axis orientated, which is pointing away from the Si micropillar surface, and positive piezoelectric polarization charges are induced at the vicinity of local pn heterojunction interface.^[23]

The corresponding piezoelectric potential is thus opposing the direction of the built-in electric field of pn junction, leading to a reduced depletion width and internal field, and enhances the injection current and emitting light intensity, subsequently.^[24] Besides, the positive piezoelectric charges effectively modify the energy band at heterojunction by reducing both the conduction and valence band of ZnO as shown in Figure 4f. Thus, more electrons are trapped at ZnO–SiO₂ interface energy barrier; meanwhile the transport of holes from Si to ZnO is hindered as well. Therefore, under compressive strains, the depletion width is reduced and more electrons from ZnO and more holes from Si are trapped at the pn heterojunction; the efficiency of recombination between electrons and holes at the heterojunction is increased and thus the light emissions are enhanced.^[20,21,25] Conversely, if the *c*-axis of ZnO nanofilm would be controlled pointing toward the interface, negative piezoelectric polarization charges are created upon compressively straining in the depletion zone. The piezoelectric field is thus in the same direction as the pn junction built-in electric field to increase the depletion region width, and the energy band of ZnO is increased at local interface to repel electrons. As a result, the recombination rate of electron holes is reduced and the light emissions are depressed.

In summary, we designed and fabricated n-ZnO nanofilm/p-Si micropillar heterostructure LED array for light emissions at room temperature. White light LEDs are achieved and characterized by EL spectrum with peaks in both visible and near-infrared regions. By introducing piezo-phototronic effect through externally applying strains, piezoelectric polarization charges presented at the vicinity of local heterojunction interface have been utilized to modify the energy band structure of ZnO and thus tune/control the transport, separation and recombination processes of photo-generated carriers. The light emission intensity of heterostructured LED array was enhanced by 120% under –0.05% compressive strains. These results indicate a promising approach to fabricate Si-based light-emitting components with high performances enhanced by piezo-phototronic effect and may represent a major step towards on-chip recording of mechanical signals by optical means, with potential applications in touchpad technology, personalized signatures, bioimaging, optical MEMS, and smart skin. Furthermore, combined with the dominate silicon microelectronic industry, large-scale device integration could be easily achieved for future assembling in silicon-based PIC and optical communication systems.

Experimental Section

Fabrication Process of Si Micropillars: P-type Si wafer was cleaned with acetone/propanol and dried in nitrogen blow at first, and then immersed into hydrofluoric acid (1%) for 2 min to remove residue organics and oxide on the surface. A layer of SiO₂ with thickness of 60 nm by dry oxidation method and a layer of Al with thickness of 100 nm were then grown on the wafer as mask. Next, a layer of Si₃N₄ with thickness of 50 nm was deposited by Plasma Enhanced Chemical Vapor Deposition (PECVD, SENTECH SI500D), followed by spin-coating and photolithography to form a layer of patterned photoresist on the surface of the Si wafer. Finally, the inductively coupled plasma (ICP) reactive ion etching (ULVAC NE-550H) was applied to produce the aligned

micropillars on the Si wafer. During the etching of Al film, Cl₂ and BCl₃ gases were introduced in the ICP chamber with flow rate of 10 and 20 sccm, respectively. During the etching of Si wafer, O₂, CF₄, and HBr gases were introduced in the chamber with the flow rate of 2, 3, and 97 sccm, respectively. At last, the wafer was washed with Al-11 aluminum etchant (H₃PO₄:CH₃COOH:HNO₃:H₂O = 72:3:3:22), deionized water and Hydrofluoric (HF) acid (1%) to remove the remnant Al and SiO₂.

Fabrication Process of LED Array: The as-fabricated Si micropillars were covered with a layer of n-type ZnO nanofilm (600 nm in thickness) by magnetron sputtering (Discovery 635, Denton Vacuum) with power of 150 W for 1.5 h. Then, a thin layer of Au nanofilm with thickness of 30 nm was sputtered on ZnO surface with power of 100 W for 10 min. Finally, the bar electrodes (Ag) or network electrodes (Au) were fabricated through lithography and deposition.

Characterization and Measurement of ZnO/Si LED Array: The ZnO/Si LED array was characterized by FESEM (field-emission scanning electron microscopy) (Hitachi SU8020) and HRTEM (high-resolution transmission electron microscopy) (FEI Tecnai G20). The ZnO/Si LED array is powered by Maynuo DC Source Meter M8812 and a pulse power supply (Agilent AFG3011C). And the optical image was taken by Zeiss Observer Z1. *I*–*V* characteristics were measured by KEITHLEY 4200SCS and the emission spectra of the device was measured by spectrometer Horiba iHR550.

Supporting Information

Supporting Information is available from the Wiley Online Library or from the author.

Acknowledgements

X.L., M.C., and R.Y. contributed equally to this work. This work was financially supported by the “thousands talents” program for pioneer researcher and his innovation team, China; National 973 Project of China (2015CB654902); Chinese National Natural Science Foundation (11374174 and 51390471); President Funding of the Chinese Academy of Sciences, National Natural Science Foundation of China (Grant Nos. 51272238, 21321062, 51432005, and 61405040); Beijing City Committee of science and technology (Z131100006013004 and Z131100006013005); the Innovation Talent Project of Henan Province (Grant No. 13HASTIT020); Talent Project of Zhengzhou University (ZDGD13001), and Surface Engineering Key Lab of Lanzhou Institute of Physics, CAST. This work made use of the resources of the National Center for Electron Microscopy in Beijing and Beijing Institute of Nanoenergy and Nanosystems, Chinese Academy of Sciences.

Received: March 7, 2015

Revised: May 23, 2015

Published online:

- [1] a) P. Ball, *Nature* **2001**, *409*, 974; b) V. R. Almeida, C. A. Barrios, R. R. Panepucci, M. Lipson, *Nature* **2004**, *431*, 1081.
- [2] V. Lien, K. Zhao, Y. Berdichevsky, Y. H. Lo, *IEEE J. Sel. Top. Quant.* **2005**, *11*, 827.
- [3] A. V. Krishnamoorthy, R. Ho, X. Z. Zheng, H. Schwetman, J. Lexau, P. Koka, G. L. Li, I. Shubin, J. E. Cunningham, *Proc. IEEE* **2009**, *97*, 1337.
- [4] S. M. Barnard, D. R. Walt, *Nature* **1991**, *353*, 338.
- [5] J. F. Wang, M. S. Gudiksen, X. F. Duan, Y. Cui, C. M. Lieber, *Science* **2001**, *293*, 1455.
- [6] Y. P. Hsieh, H. Y. Chen, M. Z. Lin, S. C. Shiu, M. Hofmann, M. Y. Chern, X. T. Jia, Y. J. Yang, H. J. Chang, H. M. Huang,

- S. C. Tseng, L. C. Chen, K. H. Chen, C. F. Lin, C. T. Liang, Y. F. Chen, *Nano Lett.* **2009**, 9, 1839.
- [7] Y. M. Huang, Q. L. Ma, B. G. Zhai, *J. Lumin.* **2013**, 138, 157.
- [8] A. Polman, *J. Appl. Phys.* **1997**, 82, 1.
- [9] N. M. Park, T. S. Kim, S. J. Park, *Appl. Phys. Lett.* **2001**, 78, 2575.
- [10] a) Y. F. Chan, W. Su, C. X. Zhang, Z. L. Wu, Y. Tang, X. Q. Sun, H. J. Xu, *Opt. Express* **2012**, 20, 24280; b) M. A. Mastro, J. D. Caldwell, R. T. Holm, R. L. Henry, C. R. Eddy, *Adv. Mater.* **2008**, 20, 115.
- [11] a) Z. Wang, R. Yu, C. Pan, Y. Liu, Y. Ding, Z. L. Wang, *Adv. Mater.* **2015**, 27, 1553; b) X. Wang, H. Zhang, R. Yu, L. Dong, D. Peng, A. Zhang, Y. Zhang, H. Liu, C. Pan, Z. L. Wang, *Adv. Mater.* **2015**, 27, 2324; c) J. Briscoe, S. Dunn, *Nano Energy* **2014**, 11, 2211.
- [12] a) C. F. Pan, Z. X. Luo, C. Xu, J. Luo, R. R. Liang, G. Zhu, W. Z. Wu, W. X. Guo, X. X. Yan, J. Xu, Z. L. Wang, J. Zhu, *ACS Nano* **2011**, 5, 6629; b) K. Q. Peng, J. J. Hu, Y. J. Yan, Y. Wu, H. Fang, Y. Xu, S. T. Lee, J. Zhu, *Adv. Funct. Mater.* **2006**, 16, 387.
- [13] W. L. Ng, M. A. Lourenco, R. M. Gwilliam, S. Ledain, G. Shao, K. P. Homewood, *Nature* **2001**, 414, 470.
- [14] S. Xu, C. Xu, Y. Liu, Y. F. Hu, R. S. Yang, Q. Yang, J. H. Ryou, H. J. Kim, Z. Lochner, S. Choi, R. Dupuis, Z. L. Wang, *Adv. Mater.* **2010**, 22, 4749.
- [15] E. Lai, W. Kim, P. D. Yang, *Nano Res.* **2008**, 1, 123.
- [16] a) W. Liu, S. L. Gu, J. D. Ye, S. M. Zhu, S. M. Liu, X. Zhou, R. Zhang, Y. Shi, Y. D. Zheng, Y. Hang, C. L. Zhang, *Appl. Phys. Lett.* **2006**, 88; b) J. D. Ye, S. L. Gu, S. M. Zhu, W. Liu, S. M. Liu, R. Zhang, Y. Shi, Y. D. Zheng, *Appl. Phys. Lett.* **2006**, 88; c) S. W. Lee, H. D. Cho, G. Panin, T. W. Kang, *Appl. Phys. Lett.* **2011**, 98.
- [17] a) K. H. Wu, C. C. Tang, S. C. Lin, in *IEEE 8th Nanotechnol. Mater. Devices Conf.*, Taiwan, **2013**, 8; b) N. Koshida, H. Koyama, *Appl. Phys. Lett.* **1991**, 30, L1221; c) F. Maier-Flaig, J. Rinck, M. Stephan, T. Bocksrocker, M. Bruns, C. Kubel, A. K. Powell, G. A. Ozin, U. Lemmer, *Nano Lett.* **2013**, 13, 475; d) K. J. Moon, T. I. Lee, W. Lee, J. M. Myoung, *Nanoscale* **2014**, 6, 3611; e) L. Canham, *Nature* **2000**, 408, 411.
- [18] F. Maier-Flaig, C. Kubel, J. Rinck, T. Bocksrocker, T. Scherer, R. Prang, A. K. Powell, G. A. Ozin, U. Lemmer, *Nano Lett.* **2013**, 13, 3539.
- [19] a) L. Pavesi, L. Dal Negro, C. Mazzoleni, G. Franzo, F. Priolo, *Nature* **2000**, 408, 440; b) A. G. Cullis, L. T. Canham, *Nature* **1991**, 353, 335.
- [20] Q. Yang, W. H. Wang, S. Xu, Z. L. Wang, *Nano Lett.* **2011**, 11, 4012.
- [21] a) C. F. Pan, L. Dong, G. Zhu, S. M. Niu, R. M. Yu, Q. Yang, Y. Liu, Z. L. Wang, *Nat. Photonics* **2013**, 7, 752; b) C. Wang, R. Bao, K. Zhao, T. Zhang, L. Dong, C. Pan, *Nano Energy* **2014**, 11, 033.
- [22] a) K. C. Pradel, W. Z. Wu, Y. S. Zhou, X. N. Wen, Y. Ding, Z. L. Wang, *Nano Lett.* **2013**, 13, 2647; b) Y. F. Hu, B. D. B. Klein, Y. J. Su, S. M. Niu, Y. Liu, Z. L. Wang, *Nano Lett.* **2013**, 13, 5026; c) C. F. Pan, R. M. Yu, S. M. Niu, G. Zhu, Z. L. Wang, *ACS Nano* **2013**, 7, 1803; d) C. F. Pan, S. M. Niu, Y. Ding, L. Dong, R. M. Yu, Y. Liu, G. Zhu, Z. L. Wang, *Nano Lett.* **2012**, 12, 3302.
- [23] Y. Wang, Q. Y. Xu, X. L. Du, Z. X. Mei, Z. Q. Zeng, Q. K. Xue, Z. Zhang, *Phys. Lett. A* **2004**, 320, 322.
- [24] Q. Yang, Y. Liu, C. F. Pan, J. Chen, X. N. Wen, Z. L. Wang, *Nano Lett.* **2013**, 13, 607.
- [25] W. Z. Wu, C. F. Pan, Y. Zhang, X. N. Wen, Z. L. Wang, *Nano Today* **2013**, 8, 619.